heritage

MDPI

Article

The Effect of Exposure Condition on the Composition of the Corrosion Layers of the San Carlone of Arona

Chiara Petiti [1], Barbara Salvadori [2], Silvia Vettori [2], Jean Marie Welter [3], Paulina Guzmán García Lascurain [1], Lucia Toniolo [1] and Sara Goidanich [1,*]

[1] Department of Chemistry, Materials and Chemical Engineering "Giulio Natta", Politecnico di Milano, Piazza Leonardo da Vinci, 32, 20133 Milano, Italy; chiara.petiti@polimi.it (C.P.); paulina.guzman@polimi.it (P.G.G.L.); lucia.toniolo@polimi.it (L.T.)
[2] Institute of Heritage Science-National Research Council (ISPC-CNR), Via Madonna del Piano, 10, 50019 Sesto Fiorentino, Italy; barbara.salvadori@cnr.it (B.S.); silvia.vettori@cnr.it (S.V.)
[3] Independent Researcher, 1361 Luxembourg, Luxembourg; jean-marie.welter@pt.lu
* Correspondence: sara.goidanich@polimi.it

Abstract: The Colossus of San Carlo Borromeo, named San Carlone for its large dimensions, represents a unique opportunity to study the long-term effects of atmospheric corrosion on patina formation on historic copper sheets. The sculpture's large dimensions, complex geometry, direct visitor interaction, and exposure conditions generate different microclimates. The purpose of this study is to understand how and to what extent these microclimates affect the formation of the copper patinas. The results show that microclimates play a key role in patina formation: in external surfaces exposed to rain, the main constituent is brochantite, whereas a wider variety of corrosion products have been found in sheltered and internal surfaces, such as antlerite, atacamite, copper oxalate, posnjakite, and anglesite.

Keywords: historic copper; patina of corrosion layers; atmospheric corrosion; cultural heritage; long term patina formation

Citation: Petiti, C.; Salvadori, B.; Vettori, S.; Welter, J.M.; Guzmán García Lascurain, P.; Toniolo, L.; Goidanich, S. The Effect of Exposure Condition on the Composition of the Corrosion Layers of the San Carlone of Arona. *Heritage* **2023**, *6*, 7531–7546. https://doi.org/10.3390/heritage6120395

Academic Editor: Fernanda Prestileo

Received: 29 September 2023
Revised: 21 November 2023
Accepted: 23 November 2023
Published: 30 November 2023

1. Introduction

Prolonged exposure to metals causes corrosion, leading to the formation of a patina on metallic surfaces, which is constituted of corrosion products and other deposit layers [1–3]. The patina's characteristics (composition, morphology, thickness, porosity, etc.) are strongly influenced by the specific environment to which the metallic surface is exposed. Also, these characteristics can significantly affect the resulting corrosion rate of the surfaces [4–6]. When dealing with cultural heritage artefacts, the conservation history of the objects, including previous conservation interventions, has a fundamental role in the patina formation and evolution.

Atmospheric corrosion poses diverse challenges to cultural heritage preservation. It can negatively impact preservation through metallic material loss and the presence of highly reactive corrosion products. Thick, dark corrosion layers could undermine the aesthetical value of artworks. Conversely, the formation of a patina could also result in a positive effect because they have been considered as a positive aesthetical feature on a series of materials (e.g., copper alloys) since ancient times. Additional historical and artistic value is given to patinas developed after decades or even centuries of exposure. Finally, some corrosion products with specific composition and/or morphologies may play an important protective role for the underlying metallic substrate.

The composition of the patina on bronze and brass materials is often composed of copper salts and minerals as corrosion products. Their composition mainly depends on the specific exposure environment. However, peculiar corrosion products have been detected due to the presence of alloying elements. Patinas formed through long-term exposure to the

environment exhibit a heterogeneous aspect, influenced by surface morphology, roughness, inclination, and exposure conditions [3,4,7]. Initially, a thin, compact, and reddish–brown layer mainly constituted by oxides is formed [7–9]. Upon further exposure, the surface layer darkens to a brown–black color that may still be constituted only of oxides [7,9]. However, the darkening might also be related to the interaction with other pollutants [8,10]. Finally, a greenish patina appears after several years of exposure, when the formation of basic copper sulphates or chlorides occurs [7,9].

Rain exposure conditions have a relevant impact on the composition and microstructure of patinas [6]. Surfaces sheltered from the rain exhibit a wider variety of copper compounds. These are characterized by a thicker layer with a higher amount of amorphous material since they are not dissolved in rain [4,6]. Conversely, under unsheltered conditions and exposed to rain washout, the observed patinas are thinner and more compact, with a lower variety of copper compounds due to rain-promoted dissolution of most soluble and less crystalline compounds.

The case study of the Colossus of San Carlo Borromeo provides an opportunity to explore the effect of over 300 years of environmental exposure on patina formation. Moreover, since it is possible to walk inside the statue up to the internal part of the head, the visitor's interaction with the sculpture can also play a role in enhancing understanding. This complexity makes the statue an interesting case study for investigating patina formation under different conditions.

The Colossus of San Carlo Borromeo, named San Carlone for its large dimensions (33 m height), is a monumental statue built between 1614 and 1698 in Arona on the Lago Maggiore (Italy). The San Carlone celebrates the Catholic Saint Carlo Borromeo (1538–1584), a prominent figure during the Counterreformation period. Specifically, this statue portrays a peculiar construction technique with an internal stone pillar supporting a wrought iron structure, covered by a "skin" of embossed copper sheets that gives the final shape to the monument. The iron structure consists of large structural iron bars fixed on the stone pillar holding a "cage" of smaller iron armatures that are in direct contact with the copper sheets. A previous study revealed that the iron elements presented a relatively noble corrosion potential, thus preventing galvanic corrosion [11].

Historical information on the statue's construction and conservation history was obtained from the archives of the Soprintendenza per I Beni Ambientali e Architettonici del Piemonte, the Veneranda Biblioteca Ambrosiana, and the Archivio Borromeo dell'Isola Bella, and published in a previous paper [12]. The statue underwent a first scarcely documented restoration in 1815–1818 and a second one in 1950 to repair the left arm that was seriously damaged during World War II. A third well-documented restoration intervention was carried out in 1974–1975, involving sandblasting of all the external copper surfaces and then re-patination. Artificial re-patination and surface protection were likely performed by using a chemical solution able to react with the surface and to favour its oxidation. Then, a protective coating was probably added. However, unfortunately, it was not possible to find details about the exact procedures and materials applied.

The San Carlo sculpture's large size, intricate geometry, and varied exposure conditions provide a unique opportunity to investigate how all these factors can influence the patina formation. This work aims to investigate the impact that microclimates have on the patina formation within the same sculpture. To do so, the patinas were characterized by their color, thickness, chemical composition, and polarization resistance.

2. Materials and Methods

2.1. Materials

An extensive in situ diagnostic campaign was carried out on representative areas of the *San Carlone* (Figure 1) by means of portable non-invasive techniques. The investigated areas are divided into *external*, referring to those of the outer section of the sculpture, and *internal*, meaning the analyzed areas inside the *San Carlone*. The external surfaces were further

divided into *exposed* and *semi-sheltered* depending on their exposure to rain. Copper microfragments and powder microsamples were also collected to perform laboratory analysis.

Figure 1. Colossus of San Carlo of Arona, named San Carlone. The white frames indicate the studied areas, while the red marks indicate the location of temperature and relative humidity sensors.

2.2. Methods

On-site measurements consisted of portable digital microscopy, portable FTIR, ultrasound measurements to detect the copper sheets' thickness, electrical conductivity measurements, and corrosion layer thickness by means of eddy currents. Laboratory analysis performed on micro-samples consisted of stereo microscopy and optical microscopy for metallographic examinations, FTIR, XRD, OES, LA-ICP-MS, and SEM-EDX. For all materials, the "bulk" copper, its surfaces, and corrosion layers were analyzed.

The microscopical analysis was performed with a portable digital microscope, i.e., Dino-Lite Premiere AM7013MT, with variable magnifications from 50× to 200×, and a Leica M205C stereomicroscope equipped with a Leica DFC 290 camera, which were implemented for on-site and laboratory analyses, respectively.

On-site FTIR characterization was performed using an FTIR Alpha spectrophotometer (Bruker Optics), with a SiC Globar source and a DTGS detector. The spectra were acquired in reflection mode and allowed for the collection of 256 scans in the 7500–375 cm^{-1} range with a resolution of 4 cm^{-1} on a 6 mm-diameter spot. The IR spectra were processed using OPUS 7.2 software. The instrument was equipped with a video camera for the selection of the area to be analyzed. Laboratory FTIR analysis was performed after dispersing the powders in KBr pellets with a Thermo Nicolet 6700 spectrophotometer and a DTGS detector with a detection range of 4000–400 cm^{-1}. One powder sample was analyzed after separating the organic residues from the inorganic part via extraction in organic solvents (first ethanol, then acetone, and finally hexane). After each step, the liquid fractions were collected and placed on a ready-made KBr pellet and allowed to evaporate.

X-ray Fluorescence measurements on-site were performed using a Niton Thermo Scientific (Waltham, MA, USA) XL2 XRF analyzer. The XRF is equipped with a Ag anode working with a voltage of 45 kV and a current of 80μA.

The XRD analysis was carried out with a PANalytical diffractometer, i.e., X'Pert PRO, with a radiation of CuKα1 = 1.54A and operating at 40 kV, 30 mA, within 2θ of 3°–70°, and equipped with an X'Celerator multidetector.

The composition of bulk copper has been evaluated on two different samples using optical emission spectroscopy (OES) and laser ablation induced coupled plasma mass spectroscopy (LA-ICP-MS). OES analyses were performed using a Spectrolab M11 OES analyzer (Spectro Analytical Instruments GmbH—Kleve, Germany) with arc spark discharge. LA-ICP-MS was carried out with a quadrupole spectrometer ICP-MS, NexION 300D (Perkin Elmer—Waltham, MA, USA), and a laser ablation system, LSX-213 (CETAC—Omaha, NE, USA), with a 213 nm UV laser (Nd:YAG, solid state, Q-switched).

The elemental composition evaluation of the bulk alloys and of corrosion layers was performed by scanning electron microscopy, coupled with microanalysis (SEM-EDX). An ESEM Zeiss EVO 50 EP in extended pressure equipped with an Oxford INCA Energy 200-Pentafet LZ4 spectrometer was used for this investigation.

On-site electrochemical measurements have been carried out to evaluate the corrosion behavior of the metallic surfaces. Linear polarization resistance (LPR) and electrochemical impedance spectroscopy (EIS) have been performed with a portable potentiostat (Ivium Technologies CompactStat—Eindhoven, The Netherlands) with the Ivium®® software version 4.993 (Ivium Technologies CompactStat—Eindhoven, The Netherlands). We employed a three electrode configuration with the same geometry of the ContactProbe proposed by Letardi [13], constituted by AISI316L stainless steel counter (CE) and pseudo-reference (RE) electrodes embedded in a PTFE case with a sponge with long "tails" soaked in an electrolyte reservoir to guarantee the constant presence of the electrolyte on the surface during the measurements. Additionally, LPR and EIS measurements have been carried out with the Minicell (Amel s.r.l—Milan, Italy) on the surfaces of the *San Carlone* and on the polished cross-section of collected micro-samples. The Minicell is constituted of a platinum counter electrode and an Ag/AgCl reference electrode, which are collectively hosted in a cylindrical plastic case where the electrolyte flows continuously due to the employment of a mini pump. The used electrolyte was an oligomineral water compound (pH of ~8 and conductivity of ~200 μS/cm) for all LPR, EIS, and E_{corr} measurements, both when using the ContactProbe and the Minicell. The LPR measurements were performed after 10 min of monitoring time (MT) of the open circuit potential (OCP). The potential varied by ±10 mV with respect to the measured E_{corr}, with a scan rate of 10 mV/min. EIS measurements were performed 10 min after the LPR measurements. The following EIS setup was adopted: a frequency range between 100 kHz and 10 mHz, ±10 mV with respect to E_{corr}, and 5 points per frequency decade. At least two repetitions of LPR and EIS analyses have been performed on each studied area. The polarization resistance (Rp) was calculated based on the LPR and EIS results. For LPR, the calculated value considered the slope of the resulting curve (on a graph E vs. i), while, for EIS measurements, it was calculated as the difference in the impedance modulus |Z| at high and low frequencies [14,15]. Such a value is inversely correlated to the corrosion resistance of the analyzed surface. On-site LPR and EIS measurements have been performed on a series of representative areas presenting surface features of the diverse conditions observed along the *San Carlone* [14,15].

Eddy current measurements were used for the evaluation of corrosion layer thickness on the Colossus of San Carlo of Arona using an Isoscope FMP30 (Helmut Fischer GmbH).

3. Results and Discussion

The analysis of the bulk copper alloy is presented as the first result and then the analysis of the surfaces and corrosion layers is discussed. This second part is divided into two sections since external and internal surfaces showed quite different features given their different exposure conditions.

3.1. Bulk Copper

Limited information is available regarding the provenance, quality, and manufacturing techniques of the metallic materials used in the construction of the *San Carlone* [12].

Compositional analysis of copper samples was performed through several techniques: OES, LA-ICP-MS, and SEM-EDX (Table 1). The results generally align well amongst dif-

ferent techniques, although some variability was observed among different samples. This variability may be ascribed to the fact that the collected samples belong to different copper sheets and that historical copper typically exhibits inherent compositional variability. The analysis revealed the presence of minor elements, such as Pb (from 0.4% to 1.45%), Sn (up to 0.4% according to SEM-EDX analysis), and Sb (up to 0.25% according to LA-ICP-MS analysis). Unfortunately, the compositional analysis did not provide enough information to formulate hypotheses on the origin of the copper ore. SEM-EDX analysis (Figure 2a,b) highlighted the presence of oxide inclusions within the copper matrix, consisting of Cu oxides (yellow circles), Pb/Sb oxides (green circles), and Sn oxides (red circles). These inclusions follow a clear orientation parallel to the surface of copper sheets, observable both through electron and optical microscopy (Figure 2). This characteristic is attributed to the manufacturing process involving hammering and embossing of the copper sheets. Metallographic observations revealed the presence of round-shaped, non-oriented (equiaxed), and twinned grains, indicating that copper plates underwent final annealing during the working process (Figure 2e,f).

Table 1. Main elements (wt%) in copper samples of the San Carlone detected with OES, LA-ICP-MS, and SEM-EDX.

	Cu	Ni	Sn	Sb	Pb
OES	99.21 ± 0.22	0.08 ± 0.06	0.09 ± 0.04	0.12 ± 0.06	0.40 ± 0.002
LA-ICP-MS	98.10	-	0.07	0.25	1.45
SEM-EDX	98.48 ± 5.90	0.08 ± 0.08	0.32 ± 0.10	0.12 ± 0.01	0.80 ± 0.13

The compositional analysis revealed high purity of the copper, with a percentage of Cu above 98.5%. This was confirmed by the on-site electrical conductivity measurements on ca. two hundred points across the statue (Figure 3).

Microscopic observation of the copper samples (Figure 2c,d) and on-site ultrasound measurements of the sheets' thickness, performed on more than 200 points (Figure 3), revealed that the copper sheets have an average thickness of around 1.2 mm. The thickness of the single plates can range between 0.7 and 2.2 mm (Figure 3). Such irregular thickness is expected considering the époque of realization and the working process.

3.2. Corrosion Layer

The corrosion layers of the *San Carlone's* copper elements were investigated in terms of morphology, color, thickness, and composition. These were studied by means of both laboratory and on-site techniques. The thickness of the corrosion layers was evaluated on more than two hundred points in all the statues by eddy currents measurements, considering both internal and external surfaces. The resulting thickness of the corrosion layers ranges between 16 and 65 µm (Figure 3), and, in 46% of the cases, the thickness ranges between 36 and 45 µm.

Furthermore, the features of the corrosion layers of the *San Carlone* were strongly dependent on their position on the monument (external or internal). Therefore, the results will be discussed separately for external and internal areas in the following text.

3.2.1. External Copper Patinas

The on-site microscopic observation of the surfaces highlighted an evident variability in the aspects of the corrosion layers (Figure 4). Black and green patinas are predominant, as expected for corrosion layers formed in outdoor environments [7,9]. Compact and adherent patinas have also been observed on unsheltered surfaces (Figure 4a–d), with no significant differences related to the surface's cardinal orientation or height. These patinas showed a typical two-layered structure, widely documented in the literature for copper natural patinas [2,4,16]. EDX analysis confirmed that the internal layer (Figure 5), normally referred to as primary patina, is mainly constituted by copper oxides, in agreement with

the literature. The outer layer (Figure 5), also known as the secondary patina, is rich in sulphur, suggesting the presence of sulphate-based compounds on the surface of the samples. Additionally, the oxide-based inclusions, observed in bulk copper, are still visible in the corrosion layers (Figure 5b). These inclusions were probably incorporated as the corrosion proceeded [17].

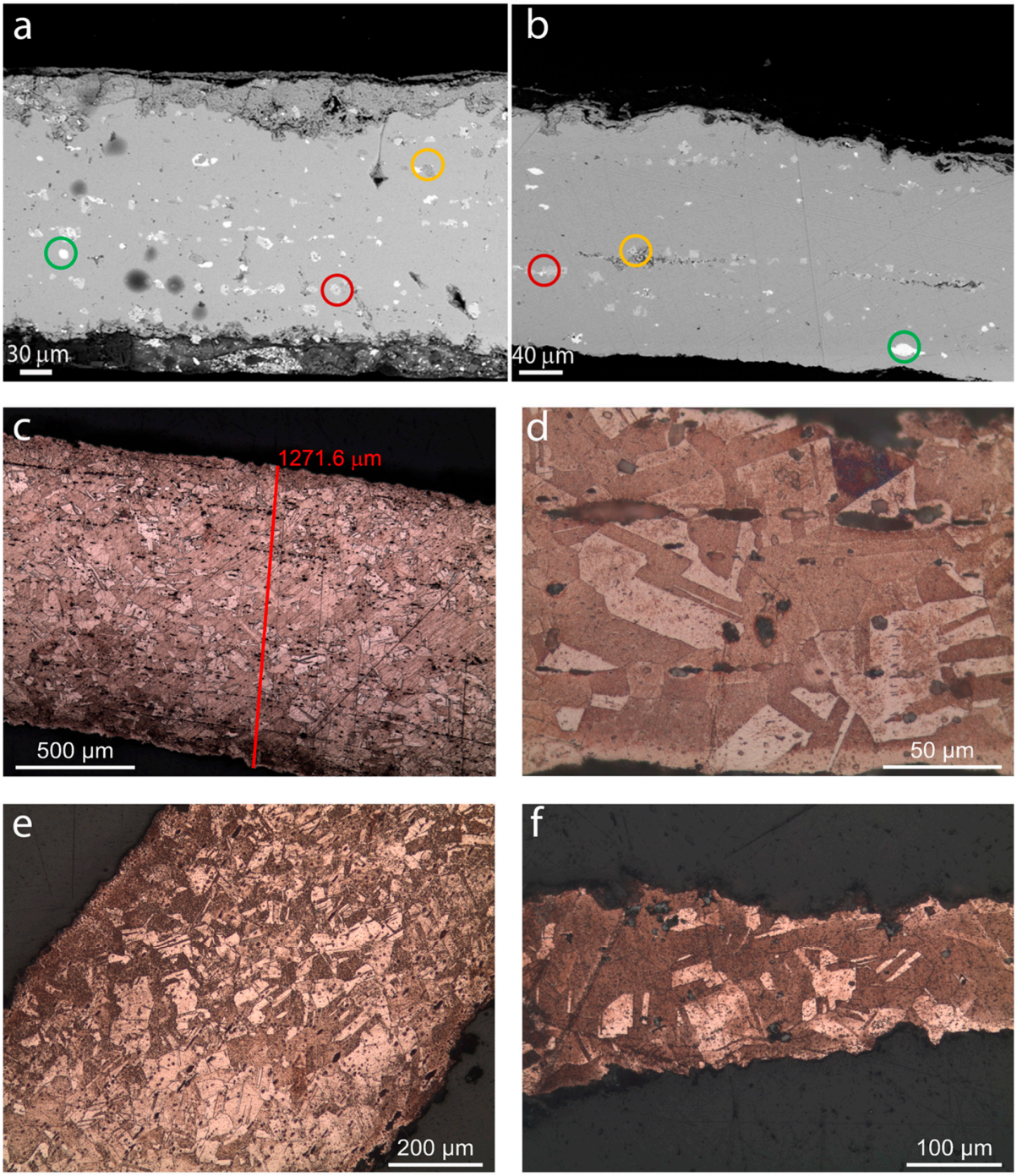

Figure 2. SEM images (**a**,**b**) of cross-section of copper samples from the San Carlone. EDX analysis revealed the composition of inclusions in the copper matrix: Cu oxide (yellow circles), Pb/Sb oxide (green circles), and Sn oxide (red circles). Optical microscopy images of cross-section of copper samples (**c**–**f**) are also included, where oriented inclusions (**c**,**d**), non-oriented inclusions (equiaxed), and round-shaped grains can be observed (**e**,**f**).

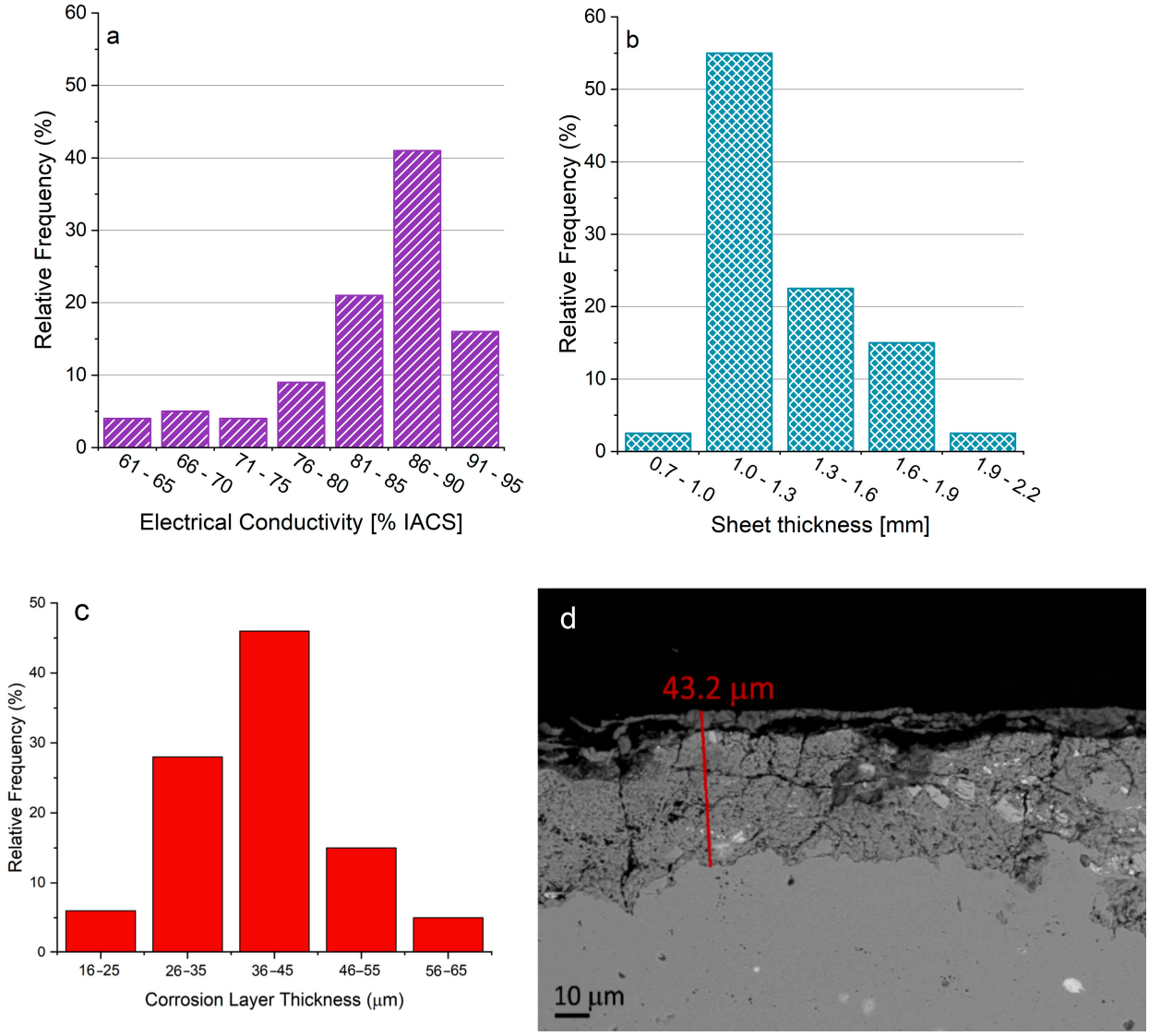

Figure 3. On-site measurements of (**a**) electrical conductivity; (**b**) thickness on the copper sheets of the San Carlone; and (**c**) thickness of corrosion layers by means of eddy currents and (**d**) SEM observations.

The chemical composition of the corrosion layers was investigated on-site using XRF and FTIR in reflection mode and in the laboratory by means of FTIR and XRD. The chemical composition resulted to be dependent on the exposure of the surfaces to the direct rain runoff. On the other hand, there was no dependence of the composition neither with cardinal orientation of the surfaces nor with their ground elevation. In Figure 6, two representative FTIR spectra are reported. FTIR revealed that brochantite ($Cu_4SO_4(OH)_6$) is the main constituent of the patina in the unsheltered surfaces and exposed to the direct action of the rain runoff areas as all its main peaks (i.e., 18) are clearly visible.

In a few cases, weak signals indicating the presence of low quantities of antlerite ($(Cu^{2+})_3SO_4(OH)_4$), atacamite ($Cu_2Cl\ (OH)_3$), or copper oxalate (CuC_2O_4) were detected. Notably, one of the most intense peaks of brochantite at 1128 cm^{-1} appears slightly shifted towards lower wavenumbers, with a broad shoulder at about 1130 cm^{-1}. This feature could be attributed to the presence of quartz and other silicate-based compounds on the surface acting as contaminants. Quartz typically displays a peak at 1080–1050 cm^{-1} and, even in a small quantity, its signal dominates over the peak of brochantite at 1128 cm^{-1}, while the weaker signal of quartz could be covered by the other brochantite peaks.

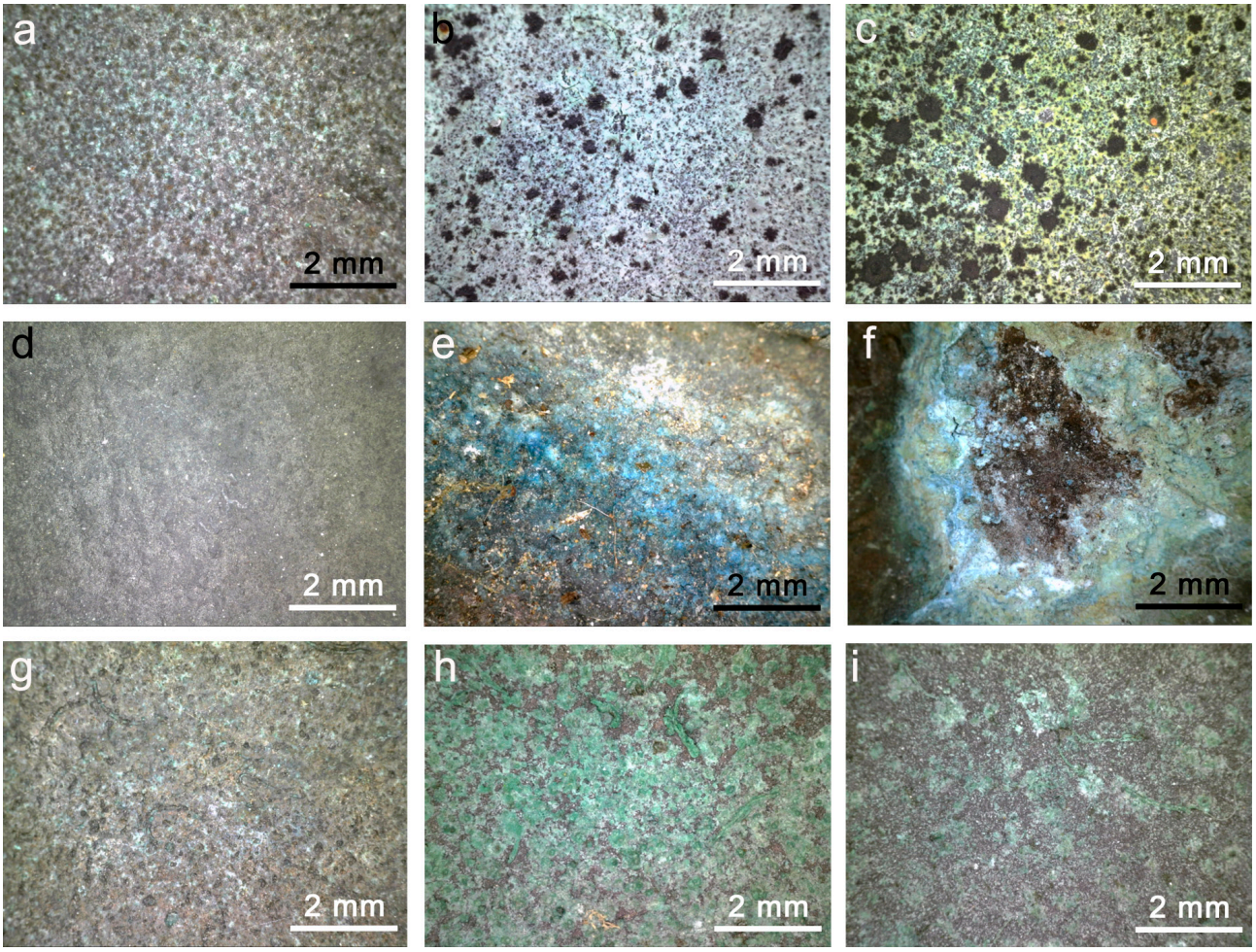

Figure 4. Portable microscopy images of surfaces of the colossus of San Carlo of Arona. (**a**–**d**): images acquired on unsheltered surfaces; (**e**,**f**): images acquired on peculiar corrosion products found only in limited and small areas; and (**g**–**i**): images acquired on sheltered areas.

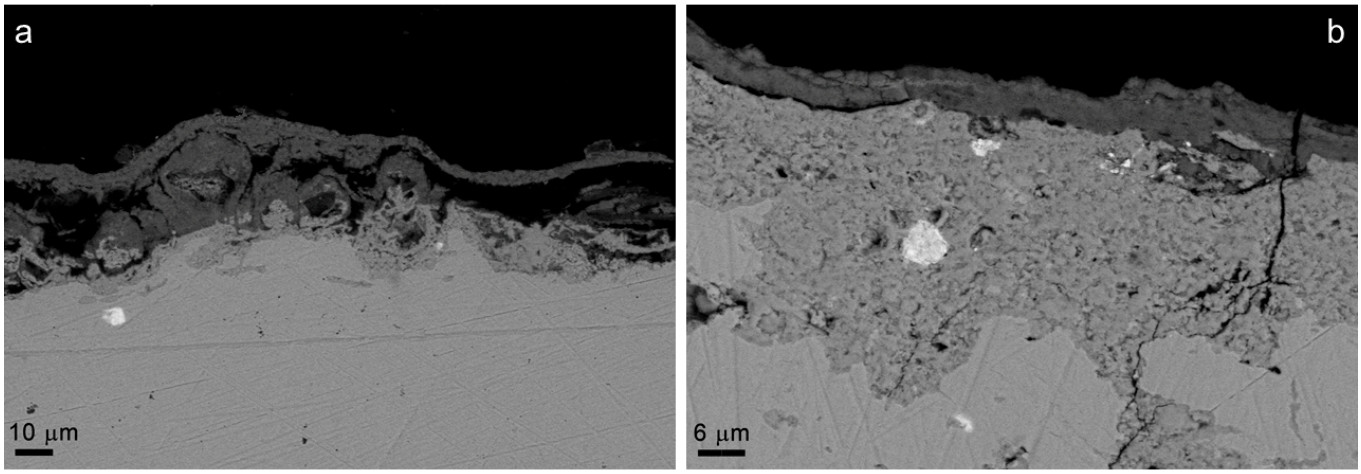

Figure 5. SEM images of cross-section of copper samples of the San Carlone: (**a**) The presence of two distinct layers (primary and secondary patinas) of corrosion products is visible. (**b**) The inclusions observed in the bulk copper are also present in the corrosion layers.

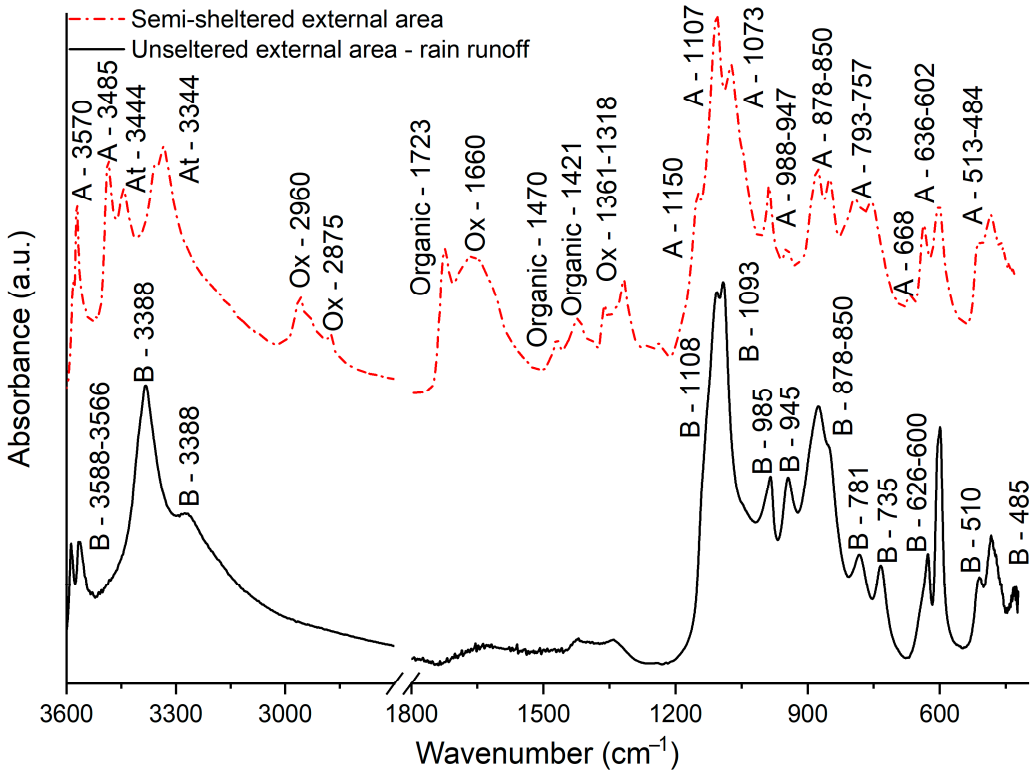

Figure 6. FTIR spectra of samples collected from the external surfaces of the San Carlone. Red line: sample collected in a semi-sheltered area; black line: sample collected in an unsheltered area. A: antlerite; B: brochantite; At: Atacamite; Ox: copper oxalate.

Antlerite was the main corrosion product detected by FTIR on sheltered and semi-sheltered surfaces. Its characteristic peaks are visible in the fingerprint region of the spectrum and at 3570 and 3485 cm^{-1} [18]. Moreover, a wider variety of corrosion products with respect to the unsheltered areas can be clearly identified. In the spectrum reported as an example in Figure 6, the distinctive signals of copper oxalate (2960, 2875, 1660, 1361, and 1318 cm^{-1}) and the main peaks of atacamite (3444 and 3344 cm^{-1}) [18] can be identified.

The predominance of different corrosion products depends on the sheltering conditions of the surfaces: brochantite is found in unsheltered areas and antlerite in sheltered ones, which can be explained by the higher solubility of antlerite (a precursor of brochantite) [4]. Brochantite is considered the most stable copper hydroxysulphate in less polluted environments. Rain action likely solubilized the antlerite on unsheltered surfaces, promoting the formation of brochantite, whereas, in sheltered areas, the transformation of antlerite into brochantite took longer. Notably, the *San Carlone* underwent an extensive restoration in 1974–1975 involving sandblasting and cleaning of the copper surfaces to remove existing corrosion layers [12,19]. Therefore, the present patina is much younger than the statue itself since it started to form in 1974–1975. The analysis did not allow for the detection or recognition of the layers related to the artificial re-patination process. It can thus be assumed that the artificial patina converted into the typical corrosion products that can be found after exposure to the atmosphere.

Despite the absence of natural sources of chlorides around Arona, the development of atacamite suggests an anthropogenic origin. The sources can be chlorides transported by the wind or the employment of chloride-based cleaning restoration treatments. Unfortunately, precise information about the exact cleaning procedure adopted is unavailable in the archive documents to confirm or exclude this hypothesis. Instead, copper oxalate formation results from the interaction between copper ions and oxalic acid, which may derive from the degradation of longer-chain organic and fatty acids. These organic acids may have an environmental origin [1,20] or arise from the interaction of the copper surfaces with organic

conservation treatments, like wax- or varnish-based protective coatings. The latter option appears quite probable as archive documents of the 1974–1975 restoration clearly report that a protective coating was applied to the entire external surface of the *San Carlone* [19,21,22]. Moreover, FTIR spectra present signals attributable to the existence of residual organic protective coatings (1723, 1470, and 1421 cm^{-1}).

The organic fraction of a powder micro-sample has been extracted and analyzed by FTIR as described in the methodology. The resulting spectrum of the extracted substances resembles the one of Paraloid (Figure 7), an acrylic-based protective coating widely diffused in the conservation field. The small differences that can be observed between the spectra are probably due to the degradation of the coating or to the use of a similar but different acrylic-based protective coating.

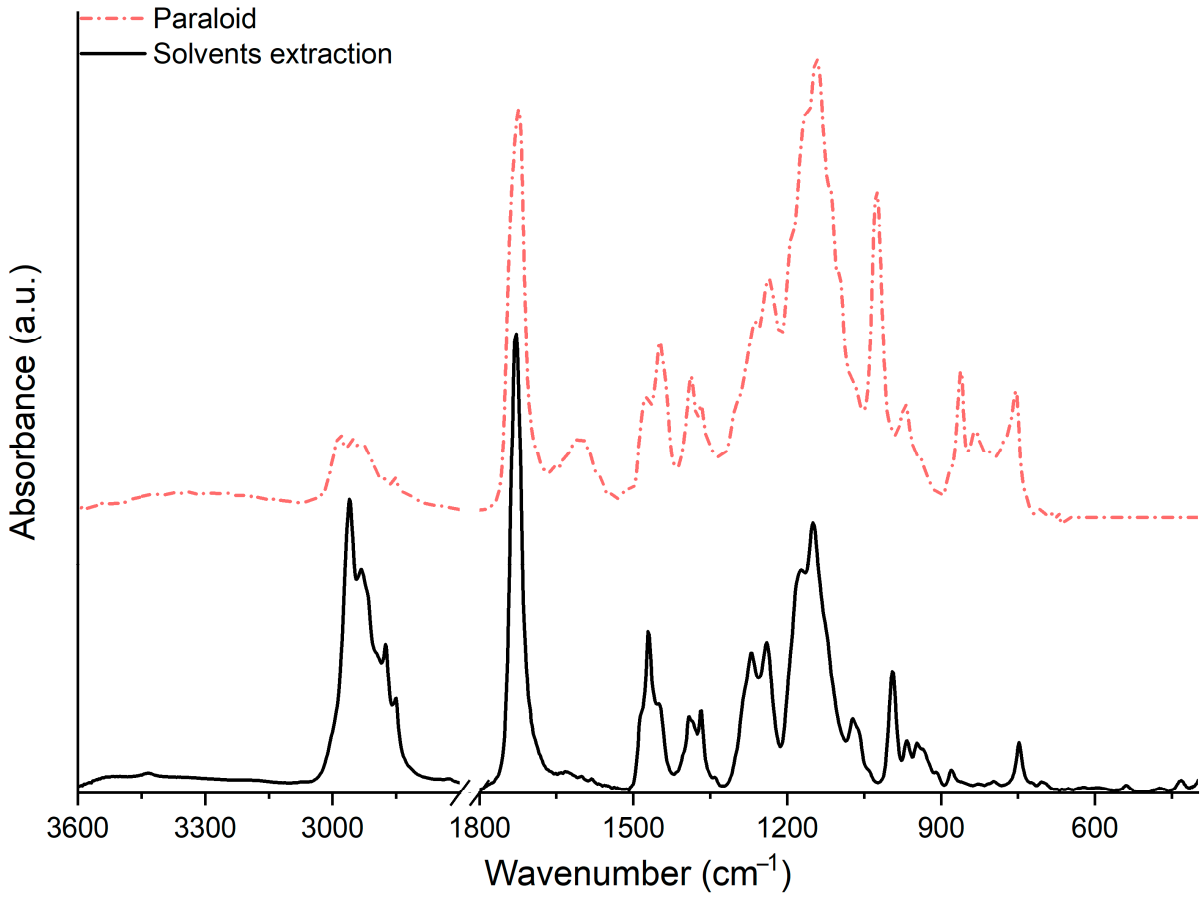

Figure 7. FTIR spectrum of organic substances extracted in acetone, ethanol, and hexane by a sample of the colossus of San Carlo of Arona with the reference spectrum of Paraloid.

XRD analysis confirmed the chemical composition of corrosion layers obtained with FTIR. Besides the copper minerals already identified by FTIR, posnjakite ($Cu_4SO_4(OH)_6 \cdot H_2O$), another copper hydroxysulphate considered as the precursor of antlerite and brochantite [4], has been recognized in the sheltered areas. Moreover, in some points, the lead sulphate anglesite ($PbSO_4$) has been identified. Its presence is rare and usually attributed to the interaction of the lead contained in the alloy with the atmosphere [17,23–25]. The presence of anglesite may also be due to environmental deposits and contaminants; actually, lead was a common pollutant up to the middle 1990s given its use for fuels.

The corrosion behavior of the external copper surfaces has been investigated by means of electrochemical measurements As can be observed in Figure 8a, the Rp values differ significantly among the studied areas, ranging from 25 $\Omega \cdot m^2$ to less than $1\Omega \cdot m^2$. On average, an Rp of about 5 $\Omega \cdot m^2$ was measured, in agreement with the Rp values reported

in the literature for non-protected copper-based surfaces exposed in a mildly aggressive environment [13,26–29]. This suggests that the coating applied during the last restoration did not provide any further protection.

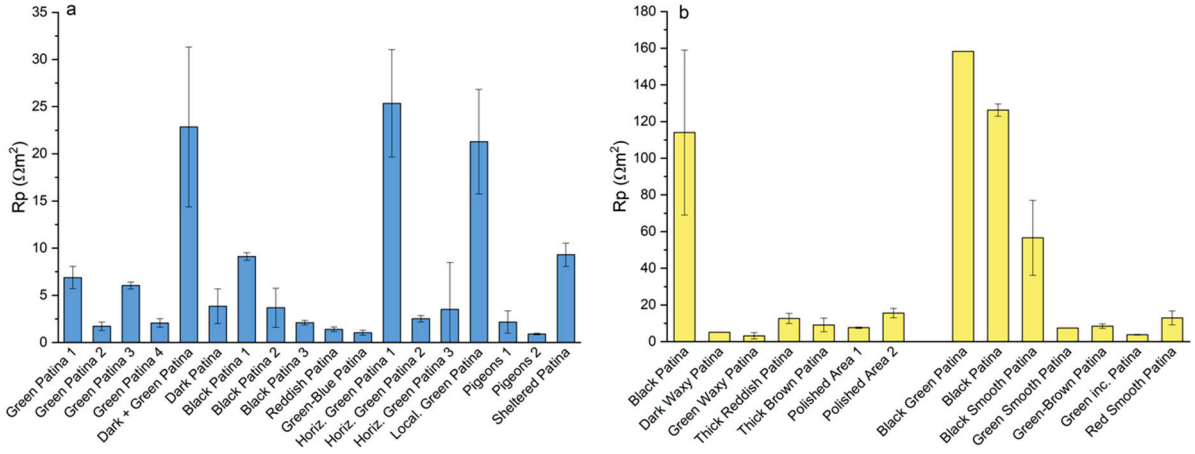

Figure 8. Results of electrochemical measurements on (**a**) external copper surfaces and (**b**) internal copper surfaces of the San Carlone: Rp values calculated from LPR and EIS measurements.

Rp values significantly lower than 5 $\Omega \cdot m^2$ have been measured in some specific cases. These low values, even lower than 1 $\Omega \cdot m^2$, correspond to the presence of relevant amounts of dejections of birds. It is known that these are corrosive substances; therefore, their effect on the corrosion behavior must be considered as wide external areas of the statue are affected by their presence. Other Rp values lower than 5 $\Omega \cdot m^2$ have also been measured in correspondence with peculiar corrosion products, observed only in a few localized areas (Figure 4e). These Rp values were obtained on some areas whose patina appeared to be uniform and stable (Figure 8a; values labelled as "green patina 2" and "4", "green-blue patina", and "reddish patina"). Such differences do not appear to be correlated to a different composition of the corrosion layers. It can be supposed then that such low protectiveness of these patinas may be related to morphological characteristics like adhesion and porosity.

The Rp value is inversely correlated to the corrosion rate of the analyzed surfaces according to Faraday's law and to the following relation:

$$i_{corr} = \frac{B}{Rp}$$

where B is a constant typical of each metal and exposure conditions.

However, it must be considered that the experimental set-up of the on-site electrochemical measurements simulates a constantly wet surface that does not represent the real condition during outdoor exposure. Thus, it is complex to obtain a precise value of corrosion rate from Rp measurements. First, only the time during which the surface is actually covered by a water film must be taken into account. This is the time of wetness (TOW) and, according to the European standard [30], it can be defined as the time during which the relative humidity is greater than 80% at a temperature greater than 0 °C. As a part of the diagnostic campaign on the *San Carlone*, the temperature (T) and relative humidity (RH) have been measured inside the statue for one year and a TOW of 26% was calculated [12]. This value is in good accordance with the 28% reported by ARPA Piemonte (Regional Agency for Environment Protection) for the Arona region [31]. The corrosion rates for the copper surfaces have also been evaluated, considering a 26% TOW and a B value of 90 mV/decade based on an average of the B values reported In the literature for Cu+ (60 mV/decade) and Cu^{2+} (120 mV/decade). Based on these assumptions, in several areas, the calculated corrosion rates exceed 5 µm/y. According to the European standard [30], these values are typical of the environments classified as extremely corrosive (CX). This is clearly not the

case here as the *San Carlone* is located in a low polluted environment, and such a high corrosion rate value would not allow the good conservation state of the monument after three centuries of exposure. Several authors have also highlighted that reliability on the definition of TOW based only on environmental data [32–34] seems to be too rough of an approximation of the time during which the conditions of active corrosion occur. Moreover, it has been highlighted that B values proposed in the literature can differ significantly from those measured experimentally [35]. In addition, a significant instantaneous acceleration of corrosion can be expected when the surface is wetted for the measurement and it is possible to assume that the corrosion rate slows down with time, leading to a lower average corrosion rate compared to the one detected during measurements. Thus, to obtain a more reliable measurement, a longer waiting time before the measurement may be considered. However, this may lead to a measurement duration that is not sustainable for on-site characterizations and a reduction of the reproducibility of results [36]. Consequently, a precise estimation of the corrosion rate could hardly be obtained and Rp should then be considered as an indicator of the surface's corrosion resistance and used mainly for comparative purposes.

3.2.2. Internal Copper Surfaces

The on-site microscopic observation of the surfaces (Figure 9) highlighted a higher variability in the aspect of the corrosion layers. In this case, the predominance of reddish, brown, or black corrosion layers can be observed. It must be highlighted that the aspect, morphology, and composition of the patinas on the internal surfaces are also strongly affected by the interaction of the visitors, particularly in the hand-touched areas affecting the aspect of the observed black (Figure 9b,e) or reddish patinas (Figure 9c). Also, a specific area, named area S and located inside the head that is completely sheltered from rain action but exposed to the external environment, has been studied due to its peculiarity. Such a surface presents apparently thick and powdery corrosion layers, characterized by a brownish (Figure 9a) or bright green (Figure 9d) color.

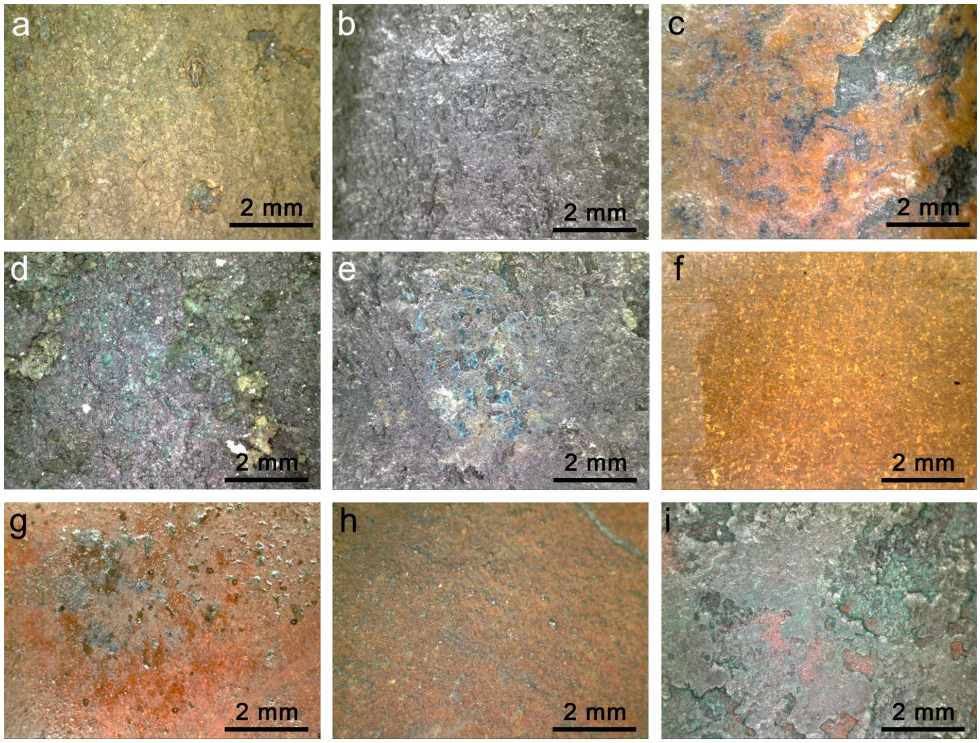

Figure 9. Portable microscopy images of surfaces of the colossus of San Carlo of Arona. (**a**–**e**): Images acquired in correspondence of an intermediate landing of the internal ladder; (**f**–**i**): images acquired on internal surfaces of the head of the statue.

The chemical composition of the corrosion layers is generally different in comparison to the ones of the external surfaces due to the presence of visitors. In general, the main corrosion product detected is antlerite. In particular, the patinas near the openings towards the outdoor show a composition similar to the external sheltered patinas: besides antlerite, the peaks related to copper oxalate are clearly visible as well as those associated with small quantities of atacamite and brochantite.

On the hand-touched areas (Figure 10), instead, a peculiar composition has been detected: besides antlerite and copper oxalate, the signals of copper stearate were clearly identified. This is probably the product of the reaction between copper ions and stearic acid, one of the most abundant fatty acids normally present on the human skin. Moreover, a higher presence of lead compounds (anglesite) with respect to the external surfaces is suggested by FTIR and XRD analysis. The presence of lead-based compounds is more relevant in correspondence to area S, characterized by thick powdery patinas, apparently heavily affected by deposition phenomena. Their presence may then have a pollution/deposition-related origin.

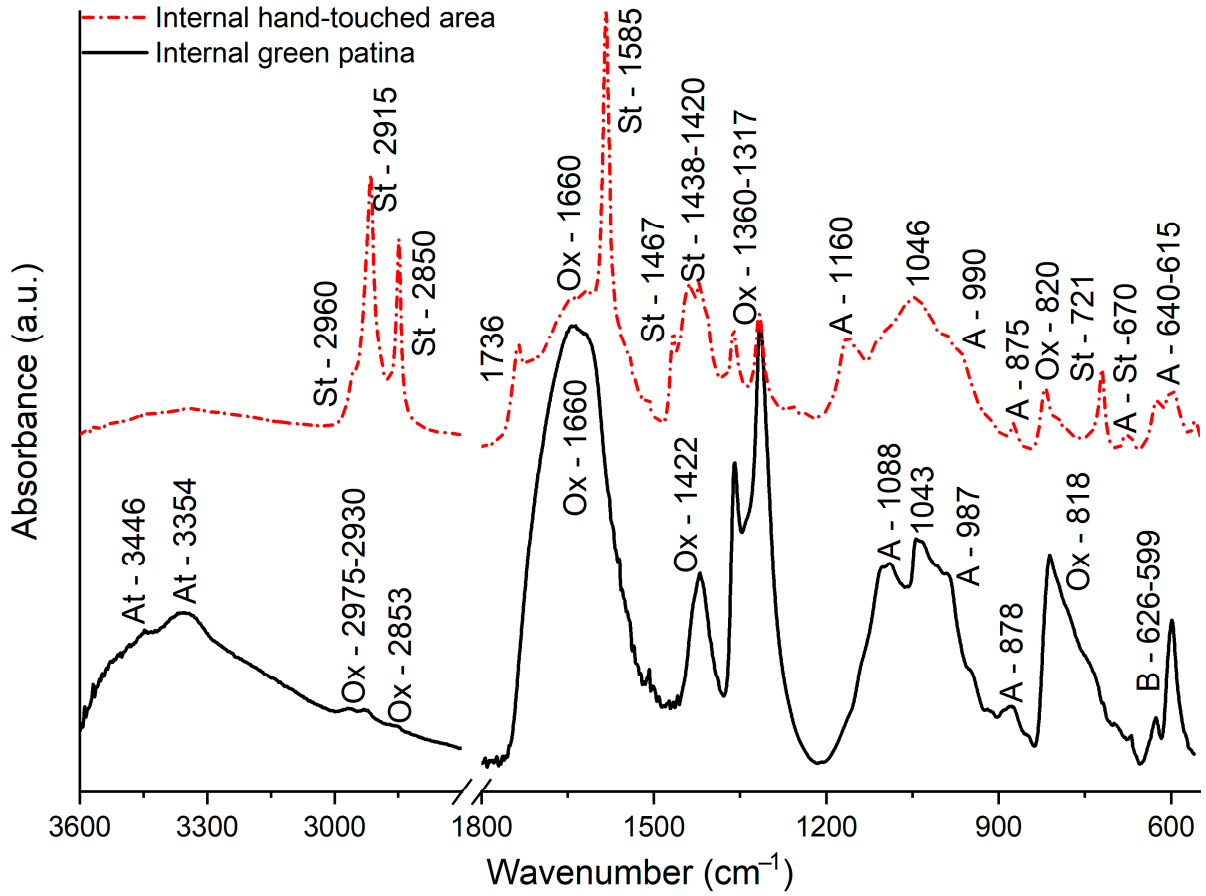

Figure 10. FTIR spectra of samples collected from the internal surfaces of the San Carlone.

The corrosion behavior of the internal surfaces was also investigated using the same methods as the external ones: on-site LPR and EIS measurements for Rp value calculation. As can be observed in Figure 8b, in many cases, Rp values between 5 and 15 $\Omega \cdot m^2$ were measured. On average, they resulted in a few $\Omega \cdot m^2$ higher than those measured on the external surfaces. Therefore, the corrosion layer formed in the internal surfaces seems to provide a slightly higher protection from corrosion compared to the external ones. In a few areas, significantly higher Rp values have been measured; these are in correspondence with black, apparently thin, patinas. Unfortunately, it was not possible to correlate such peculiar corrosion behavior to the composition or to the morphology of the patinas.

4. Conclusions

The study and characterization of the internal and external surfaces of the *San Carlone* of Arona confirmed that the exposure conditions and micro-climates can influence the state of conservation of metallic artefacts as they strongly influence the patina formation, even in the same sculpture. The exposure conditions are a consequence of the complex structure and geometry of the monument, allowing the formation of a wide variety of corrosion products.

External–unsheltered areas predominantly exhibit brochantite, while external–sheltered and semi-sheltered areas show a wider variety of corrosion products, including more soluble and less stable copper compounds like antlerite and traces of atacamite. The chemical composition of internal surfaces is also affected by the presence of visitors inside the monument, with corrosion products similar to external–sheltered surfaces as well as copper salts of fatty acids present on hand-touched surfaces. Notably, the presence of the lead sulphate anglesite, potentially linked to pollution, has been observed on surfaces exposed to wind but sheltered by rain.

Author Contributions: Conceptualization, C.P., J.M.W. and S.G.; data curation, C.P. and S.G.; formal analysis, C.P., B.S., S.V. and J.M.W.; funding acquisition, J.M.W. and S.G.; investigation, C.P., B.S., J.M.W. and S.G.; methodology, C.P. and S.G.; project administration, S.G.; resources, S.V., J.M.W. and S.G.; supervision, J.M.W., L.T. and S.G.; validation, C.P. and S.G.; visualization, C.P., P.G.G.L. and S.G.; writing—original draft, C.P. and S.G.; writing—review and editing, C.P., B.S., S.V., J.M.W., P.G.G.L., L.T. and S.G. All authors have read and agreed to the published version of the manuscript.

Funding: This research was funded by the European Copper Institute (ECI), project number MDP-25629-central-54208 04-08-17 and the agreement of donation for the "non-invasive corrosion investigations on the monument of San Carlo Borromeo" Arona–Lago Maggiore by the Helmut Fischer Stiftung Foundation signed on 21 November 2017.

Data Availability Statement: Data will be made available upon reasonable request.

Acknowledgments: The authors are grateful to the European Copper Institute (ECI) for the financial support of the research activities and to Helmut-Fischer-Stiftung for the financial support and for lending analytical equipment. The authors also want to thank the Veneranda Biblioteca Ambrosiana, owner of the San Carlone, especially to Gianluca Erba for having allowed the performance of the diagnostic activity, providing logistic support, as well as for their permission to access their archive documents. The authors are also grateful to the Soprintendenza per I Beni Ambientali e Architettonici del Piemonte, which oversees the safeguard of the San Carlone, for the collaboration and support during the research. They also thank the historical archive Archivio Borromeo dell'Isola Bella for having provided the possibility of examining their historical documents. The authors are also thankful to Sergio Bonazzi from Sirio Analytics, Hendrik Busch from Mansfelder Kupfer und Messing (MKM), and Sébastien Cremel from Arcelor Mittal for their precious contributions to the diagnostic activity on the San Carlone. We are grateful to Romina Paris for her enthusiastic and precious contribution to the archive activity. Lastly, the authors remember with great esteem Jean Marie Welter, without whom this research would not have been possible. We would like to thank his great contributions to the experimental part, analysis, and discussion of the results and paper drafting.

Conflicts of Interest: The authors declare no conflict of interest.

References

1. Graedel, T.E.; Nassau, K.; Franey, J.P. Copper Patinas Formed in the Atmosphere—I. Introduction. *Corros. Sci.* **1987**, *27*, 639–657. [CrossRef]
2. Chiavari, C.; Rahmouni, K.; Takenouti, H.; Joiret, S.; Vermaut, P.; Robbiola, L. Composition and Electrochemical Properties of Natural Patinas of Outdoor Bronze Monuments. *Electrochim. Acta* **2007**, *52*, 7760–7769. [CrossRef]
3. Scott, D.A. *Copper and Bronze in Art: Corrosion, Colorants, Conservation*; Getty Publications: Los Angeles, CA, USA, 2002; ISBN 0892366389.
4. Leygraf, C.; Wallinder, I.O.; Tidblad, J.; Graedel, T. *Atmospheric Corrosion*; John Wiley & Sons: Hoboken, NJ, USA, 2016; ISBN 1118762274.

5. Arceo-Gómez, D.E.; Reyes-Trujeque, J.; Zambrano-Rengel, G.E.; Pérez-López, T.; Orozco-Cruz, R. Electrochemical Characterization of Patinas Formed on a Historic Bell from the Cathedral Museum of Campeche-México, World Heritage Site. *Int. J. Electrochem. Sci.* **2016**, *11*, 9379–9393. [CrossRef]
6. Krätschmer, A.; Wallinder, I.O.; Leygraf, C. The Evolution of Outdoor Copper Patina. *Corros. Sci.* **2002**, *44*, 425–450. [CrossRef]
7. FitzGerald, K.P.; Nairn, J.; Skennerton, G.; Atrens, A. Atmospheric Corrosion of Copper and the Colour, Structure and Composition of Natural Patinas on Copper. *Corros. Sci.* **2006**, *48*, 2480–2509. [CrossRef]
8. Knotkova, D.; Kreislova, K. Atmospheric Corrosion and Conservation of Copper and Bronze. *WIT Trans. State Art Sci. Eng.* **2007**, *28*, 107–142.
9. Leygraf, C.; Chang, T.; Herting, G.; Wallinder, I.O. The Origin and Evolution of Copper Patina Colour. *Corros. Sci.* **2019**, *157*, 337–346. [CrossRef]
10. Strandberg, H.; Johansson, L. The Formation of Black Patina on Copper in Humid Air Containing Traces of SO_2. *J. Electrochem. Soc.* **1997**, *144*, 81. [CrossRef]
11. Petiti, C.; Martini, C.; Chiavari, C.; Vettori, S.; Welter, J.M.; Guzmán García Lascurain, P.; Goidanich, S. The San Carlo Colossus: An Insight into the Mild Galvanic Coupling between Wrought Iron and Copper. *Materials* **2023**, *16*, 2072. [CrossRef]
12. Petiti, C.; Pistidda, S.; Welter, J.M.; Toniolo, L.; Giambruno, M.; Goidanich, S. Learning from History: The Case of the San Carlone Colossus after the Test of Time. *J. Inst. Conserv.* **2022**, *45*, 18–35. [CrossRef]
13. Letardi, P. Laboratory and Field Tests on Patinas and Protective Coating Systems for Outdoor Bronze Monuments. In Proceedings of the International Conference on Metals Conservation, Canberra, Australia, 4–8 October 2004; Volume 48, p. 379387.
14. Zhang, X.; He, W.; Wallinder, I.O.; Pan, J.; Leygraf, C. Determination of Instantaneous Corrosion Rates and Runoff Rates of Copper from Naturally Patinated Copper during Continuous Rain Events. *Corros. Sci.* **2002**, *44*, 2131–2151. [CrossRef]
15. Nishikata, A.; Zhu, Q.; Tada, E. Long-Term Monitoring of Atmospheric Corrosion at Weathering Steel Bridges by an Electrochemical Impedance Method. *Corros. Sci.* **2014**, *87*, 80–88. [CrossRef]
16. Robbiola, L.; Blengino, J.-M.; Fiaud, C. Morphology and Mechanisms of Formation of Natural Patinas on Archaeological Cu–Sn Alloys. *Corros. Sci.* **1998**, *40*, 2083–2111. [CrossRef]
17. Morcillo, M.; Chang, T.; Chico, B.; de la Fuente, D.; Wallinder, I.O.; Jiménez, J.A.; Leygraf, C. Characterisation of a Centuries-Old Patinated Copper Roof Tile from Queen Anne's Summer Palace in Prague. *Mater. Charact.* **2017**, *133*, 146–155. [CrossRef]
18. Catelli, E.; Sciutto, G.; Prati, S.; Jia, Y.; Mazzeo, R. Characterization of Outdoor Bronze Monument Patinas: The Potentialities of near-Infrared Spectroscopic Analysis. *Environ. Sci. Pollut. Res.* **2018**, *25*, 24379–24393. [CrossRef] [PubMed]
19. Ferrari Da Passano, C. *Restauro Statico, Estetico e Conservativo Del Colosso Di San Carlo–Arona*; Allegato, A., Ed.; Amministrazione della Fabbrica del Duomo di Milano: Milano, Italy, 1975.
20. Tétreault, J.; Cano, E.; van Bommel, M.; Scott, D.; Dennis, M.; Barthés-Labrousse, M.-G.; Minel, L.; Robbiola, L. Corrosion of Copper and Lead by Formaldehyde, Formic and Acetic Acid Vapours. *Stud. Conserv.* **2003**, *48*, 237–250. [CrossRef]
21. *Preventivo per Opere Di Pulitura, Patinatura e Protezione Della Statua Di San Carlo, Arona*; Taiko, 1973.
22. *Invoice n. 14/75—"Fattura per Opere Di Verniciatura per Restauro Colosso Di San Carlo, Arona*; IRIDE: Orlando, FL, USA, 1975.
23. Chiavari, C.; Bernardi, E.; Martini, C.; Passarini, F.; Ospitali, F.; Robbiola, L. The Atmospheric Corrosion of Quaternary Bronzes: The Action of Stagnant Rain Water. *Corros. Sci.* **2010**, *52*, 3002–3010. [CrossRef]
24. Ingo, G.M.; Riccucci, C.; Giuliani, C.; Faustoferri, A.; Pierigè, I.; Fierro, G.; Pascucci, M.; Albini, M.; Di Carlo, G. Surface Studies of Patinas and Metallurgical Features of Uncommon High-Tin Bronze Artefacts from the Italic Necropolises of Ancient Abruzzo (Central Italy). *Appl. Surf. Sci.* **2019**, *470*, 74–83. [CrossRef]
25. Bernabale, M.; Nigro, L.; Montanari, D.; Niveau-de-Villedary, A.M.; De Vito, C. Microstructure and Chemical Composition of a Sardinian Bronze Axe of the Iron Age from Motya (Sicily, Italy). *Mater. Charact.* **2019**, *158*, 109957. [CrossRef]
26. Bartolini, M.; Colombo, B.; Marabelli, M.; Marano, A.; Parisi, C. Non-Destructive Tests for Control of Ancient Metallic Artifacts. In Proceedings of the Metal 95: Proceedings of the International Conference on Metals Conservation, Semur-en-Auxois, France, 25–28 September 1995; pp. 43–49.
27. Gulotta, D.; Mariani, B.; Guerrini, E.; Trasatti, S.; Letardi, P.; Rosetti, L.; Toniolo, L.; Goidanich, S. "Mi Fuma Il Cervello" Self-Portrait Series of Alighiero Boetti: Evaluation of a Conservation and Maintenance Strategy Based on Sacrificial Coatings. *Herit. Sci.* **2017**, *5*, 1–13. [CrossRef]
28. Joseph, E.; Letardi, P.; Rocco, M.; Prati, S.; Vandini, M. Innovative Treatments for the Protection of Outdoor Bronze Monuments. In Proceedings of the Interim Meeting of the ICOM-CC Metal WG, Amsterdam, The Netherlands, 17–21 September 2007; pp. 71–77.
29. Goidanich, S.; Toniolo, L.; Jafarzadeh, S.; Wallinder, I.O. Effects of Wax-Based Anti-Graffiti on Copper Patina Composition and Dissolution during Four Years of Outdoor Urban Exposure. *J. Cult. Herit.* **2010**, *11*, 288–296. [CrossRef]
30. *ISO–ISO 9223:2012*; Corrosion of Metals and Alloys—Corrosivity of Atmospheres—Classification, Determination and Estimation. International Organization for Standardization: Geneva, Switzerland, 2012.
31. Agenzia Regionale per La Protezione Dell'Ambiente Della Lombardia. Available online: https://www.arpalombardia.it/Pages/ARPA_Home_Page.aspx (accessed on 21 March 2023).
32. Schindelholz, E.; Kelly, R.G.; Cole, I.S.; Ganther, W.D.; Muster, T.H. Comparability and Accuracy of Time of Wetness Sensing Methods Relevant for Atmospheric Corrosion. *Corros. Sci.* **2013**, *67*, 233–241. [CrossRef]
33. Schindelholz, E.; Kelly, R.G. Wetting Phenomena and Time of Wetness in Atmospheric Corrosion: A Review. *Corros. Rev.* **2012**, *30*, 135–170. [CrossRef]

34. Morales, J.; Martín-Krijer, S.; Díaz, F.; Hernández-Borges, J.; González, S. Atmospheric Corrosion in Subtropical Areas: Influences of Time of Wetness and Deficiency of the ISO 9223 Norm. *Corros. Sci.* **2005**, *47*, 2005–2019. [CrossRef]
35. Rosetti, L. In-Situ Non-Destructive Monitoring Techniques and Protective Coatings for Copper Alloys Artefacts of Cultural Heritage. Master's Thesis, Politecnico di Milano, Milan, Italy, 2015.
36. Petiti, C.; Gulotta, D.; Mariani, B.; Toniolo, L.; Goidanich, S. Optimisation of the Setup of LPR and EIS Measurements for the Onsite, Non-Invasive Study of Metallic Artefacts. *J. Solid State Electrochem.* **2020**, *24*, 3257–3267. [CrossRef]